Description of the Eulerian Acid Deposition Model

Jerzy Bartnicki, Krzysztof Olendrzynski, Jan Eiof Jonson, Erik Berge and Steffen Unger[+]

The Eulerian acid deposition model has been developed at MSC-W as a multi-layer model for simulating atmospheric transport and deposition of nitrogen and sulphur compounds in Europe. The first version of the EMEP Eulerian model was developed by Berge (1993a) and then modified and further improved by Jakobsen *et al.* (1995). At this stage, the model was called MADE50 - Multi-level Acid Deposition model for Europe with 50 km resolution. Nitrogen chemistry was introduced into the model by Jonson and Berge (1995) and a new dry deposition module for SO_2, NO_2, HNO_3 and NH_3 was implemented by Jakobsen *et al.*, (1996). The MADE50 model was run for 1992 and the results compared with measurements available from the EMEP stations in Europe (Jakobsen *et al.*, 1995; Jonson *et al.*, 1998a, 1998b). Model validation for 1996 data is described in Olendrzynski *et al.*, (1998).

The development of the MADE50 model has been documented in many publications (e.g. Berge, 1993a; Jakobsen *et al.*, 1995; Jonson and Berge, 1995; Jakobsen *et al.*, 1996; Jakobsen *et al.*, 1997; Berge, 1997; Berge and Jakobsen, 1998). In the description of the MADE50 model given below a comprehensive picture of the latest model version is presented.

1 Basic model equations

Concentrations of nine chemical components are computed in the latest version of the MADE50 model: NO, NO_2, PAN, HNO_3, NH_4NO_3, SO_4, SO_2 and $[(NH_4)_2SO_4+NH_4HSO_4]/2$ further referred as $(NH_4)_{1.5}SO_4$. Derivation of the basic model equation describing: emission, atmospheric transport, diffusion, chemical transformations and deposition of one of the selected compounds in the σ-coordinate system can be found in Jakobsen *et al.* (1995). This equation, formulated in the Polar Stereographic Projection at 60^oN has the following form:

$$\frac{\partial(\psi p^*)}{\partial t} + m^2\frac{\partial\left(\frac{u}{m}\psi p^*\right)}{\partial x} + m^2\frac{\partial\left(\frac{v}{m}\psi p^*\right)}{\partial y} + \frac{\partial(\sigma\psi p^*)}{\partial\sigma} = \tag{1}$$

$$= \left[\frac{g}{p^*}\right]^2\frac{\partial}{\partial\sigma}\left[\rho^2 K_z\frac{\partial}{\partial\sigma}(\psi p^*)\right] + \frac{p^*}{\rho}S$$

[+]Institute for Computer Architecture (FIRST) of the German Association for Mathematics and Data Processing (GMD), Berlin, Germany.

where ψ is the mixing ratio of pollutant mass to air mass; *(u,v)* are horizontal components of the velocity field; *m* - is the map factor for the Polar Stereographic Projection at 60^{o}N; g is the gravitational acceleration; ρ is the air density; K_z is the coefficient of vertical diffusion and *S* represents all source and sink terms, including chemical transformation. The vertical coordinate σ is defined as:

$$\sigma = \frac{p - p_T}{p^*} \tag{2}$$

where $p^* = p_s - p_T$; p is the pressure at σ level; p_s is the surface pressure and p_T = 100 hPa represents the pressure at the top of the model domain. In Equation (1), $\dot{\sigma} = \frac{d\sigma}{dt}$, is the vertical velocity.

1.2 Advection and diffusion

Second, third and fourth term in the Equation (1) represent advection of every pollutant in the x-horizontal, y-horizontal and σ-vertical direction, respectively.

Horizontal diffusion is not calculated in the model because a small amount of the numerical diffusion is already introduced by the advection algorithm. Parameterization of vertical diffusion is the same as in the numerical weather prediction model LAM50E (Jakobsen *et al.*, 1995), which was used to produce input meteorological data for the MADE50 model. The vertical diffusion coefficient, K_z, is derived from the surface drag coefficient (Luis, 1979) in the surface layer but is only used for computing dry deposition fluxes. Above the surface layer this coefficient is calculated based on an the empirical formula suggested by Blackadar (1979) where the mixing length and the local bulk Richardson Number are the most important parameters:

$$K_z = l^2 \cdot \left| \frac{\partial \overrightarrow{V_H}}{\partial z} \right| \cdot F(Ri) \tag{3}$$

where $\overrightarrow{V_H} = (u, v)$ is the horizontal velocity and the turbulent mixing length, *l*, is parameterized according to Nordeng (1986):

$$l = \begin{cases} \kappa \cdot z & z \le z_m \\ \kappa \cdot z_m & z > z_m \end{cases} \tag{4}$$

In Equation (A2.4) κ is von Karman constant (κ=*0.35*), *z* is the height above the ground and z_m=200 m. The local bulk Richardson Number in the layer of thickness, Δz, is defined as:

$$Ri = \frac{g}{\theta} \cdot \frac{\left(\frac{\Delta\theta}{\Delta z}\right)}{\left(\frac{\Delta \overrightarrow{V_H}}{\Delta z}\right)^2} = \frac{g \cdot \Delta z \cdot \Delta\theta}{\theta \cdot (\Delta \overrightarrow{V_H})^2} \tag{5}$$

where $(\Delta \overrightarrow{V_H})^2 = (\Delta u)^2 + (\Delta v)^2$ and for an arbitrary state variable q, $\Delta q = q(z + \Delta z) - q(z)$. Following Nordeng (1986), critical Richardson Number is defined as

$$Ri_c = A \cdot \left(\frac{\Delta z}{\Delta z_0}\right)^B \tag{6}$$

where $A = 0.115, B = 0.175$ and $\Delta z_0 = 0.01m$. Atmosphere is turbulent when $Ri < Ri_c$. The local eddy diffusivity coefficient is calculated in the model using the following formula:

$$K_z = l^2 \cdot \left|\frac{\Delta \overrightarrow{V_H}}{\Delta z}\right| \cdot F(Ri) \tag{7}$$

where:

$$F(Ri)) = \begin{cases} \sqrt{1.1 - 87 \cdot Ri} & Ri \le 0 \\ 1.1 - 1.2 \cdot Ri/Ri_c & 0 < Ri \le 0.5 \cdot Ri_c \\ 1.0 - Ri/Ri_c & 0.5 \cdot Ri_c < Ri \le Ri_c \end{cases} \tag{8}$$

In the sigma coordinates, diffusion coefficient has the following form:

$$K_\sigma = K_z \cdot \rho^2 \cdot \left(\frac{g}{p^*}\right) \tag{9}$$

1.3 Emissions

Emissions are the most important component on the right-hand side of Equation (1) representing source and sink terms for the pollutants. The 1996 emission input to the Eulerian acid deposition model consitsts of gridded annual totals of high and low-level SO_2, NO_x and NH_3. Low-level emissions (below 100 m) are injected into the lowest model layer (below approximately 90 m) and high-level emissions are split between the second, third and fourth model layer above the surface, in proportions 25%, 50% and 25%, respectively. For most of the European countries emission inventories in the 50 km grid are based on data officially reported to

EMEP by individual countries, however, expert estimates are also used for certain regions in Europe. Seasonal variability of the emissions is parameterized in the model. For SO_2 and NO_x the GENEMIS country-specific database was used to define proportions of the total annual emissions in each month (Barret and Berge, 1996). For ammonia, emissions are distributed throughout the year with a sine function with 30% amplitude, and an assumed peak in summer. Marine biogenic sulphur emissions vary with season and latitude with a maximum rate in the North Sea in spring and a minimum in winter (Tarrason and Iversen, 1998). Full description of the EMEP emission inventories for 1996 can be found in the main report.

1.4 Dry deposition

Dry and wet depositions are the most important processes in removing pollutants from the atmosphere. A detailed description of the dry deposition parameterization used in the present version of the model is given in the EMEP reports (Jonson and Berge, 1995; Jakobsen *et. al.* 1996, 1997).

In the surface boundary layer (SBL), the dry deposition flux, *F*, can be described by the following expression:

$$F = V_d(z) \cdot [c(z) - c_s] \tag{10}$$

where *c(z)* is the concentration of pollutant at height *z*; c_s is the concentration of pollutant at the surface and $V_d(z)$ is the dry deposition velocity at height *z*. If the surface is covered by vegetation, a zero-plane displacement, *d*, is included into Equation (A2.10): $z \rightarrow z - d$. For the absorbing surface, the c_s=0.

For particles: NH_4NO_3, $(NH_4)_{1.5}SO_4$ and SO_4 the dry deposition velocity is constant in the MADE50 model and equal to 0.1 *cm* s^{-1}. For gases: NO_2, PAN, HNO_3, NH_3 and SO_2, the resistance analogy is used in the parameterization of the dry deposition velocity in Equation (A2.10):

$$V_d = (r_a + r_b + r_s)^{-1} \tag{11}$$

where r_a is the surface layer aerodynamic resistance; r_b is quasi-laminar or viscous-sublayer resistance and r_s is the surface resistance. The units of all these resistances are *s* m^{-1}.

1.4.1 Aerodynamic resistance

The SBL resistance to turbulent transport of heat and trace gas is given by the following equation:

$$r_a(z) = \frac{1}{\kappa u_*}\left[\ln\left(\frac{z-d}{z_0}\right) - \Psi_m\left(\frac{z-d}{L}\right) + \Psi_h\left(\frac{z_0}{L}\right)\right] \tag{12}$$

Here u_* is the friction velocity, z_0 is the roughness length, L is the Monin-Obukhov length and κ is von Karman's constant. The roughness length and the displacement height are assumed to be 10% and 70% of the vegetation height, respectively. In all the calculations, Ψ_m and Ψ_h are the similarity functions for momentum and heat, respectively:

$$\begin{aligned}
\Psi_m(\xi) &= \ln\left[\left(\frac{1+(1-15\xi)^{0.5}}{2}\right)\left(\frac{1+(1-15\xi)^{0.25}}{2}\right)^2\right] - 2\,\mathrm{atan}\left(1+(1-15\xi)^{0.25}\right) + \frac{\pi}{2} \\
\Psi_h(\xi) &= 2\ln\left[\frac{1+(1-15\xi)^{0.5}}{2}\right] \qquad for \quad L<0 \\
\Psi_h(\xi) &= \Psi_m(\xi) = -5\xi \qquad for \quad L \geq 0
\end{aligned} \tag{13}$$

in which $\xi = (z-d)/L$ or $\xi = z_0/L$.

From the weather prediction model LAM50E only average grid cell values of u_*, T_*, L and z_0 are available for the dry deposition module. However, in the dry deposition module atmospheric resistances in each EMEP grid cell are calculated first for every land use type. Therefore, a special algorithm (Jakobsen *et al.*, 1996) was developed to convert grid averaged values of the key variables to land use specific variables. This algorithm is described by the set of equations given below:

$$\tilde{u}_* = \sqrt{\frac{\tau}{\tilde{\rho}_s}} \tag{14}$$

where $\tilde{u}_*$ is the friction velocity calculated form the LAM50E model, τ is the turbulent stress and $\tilde{\rho}_s$ is the density of dry air at the surface.

$$\tilde{T}_* = \frac{-\tilde{H}_d}{c_p \cdot \tilde{\rho}_s \cdot \tilde{u}_*} \tag{15}$$

$$\tilde{L} = \frac{\tilde{u}_*^2 \cdot \tilde{\theta}_s}{\kappa \cdot g \cdot \tilde{\theta}_*} = \frac{\tilde{u}_*^2 \cdot \tilde{T}_s}{\kappa \cdot g \cdot \tilde{T}_*} \tag{16}$$

In Equations (15) and (16), $\tilde{T}_*$ and $\tilde{L}_*$ are respectively, scaling temperature and Monin-Obukhov length from the LAM50E model; $\tilde{H}_d$ is the turbulent heat flux, $\tilde{\theta}_s$ and $\tilde{T}_s$ a potential temperature and temperature at the surface, respectively, from the LAM50E model; c_p is the specific heat at constant pressure for dry air.

The land use type specific friction velocities u_*, specific scaling temperatures T_* and specific

Monin-Obukhov lengths L are calculated as follows:

$$u_* = \tilde{u}_* \cdot \frac{\ln\left(\frac{z-d}{\tilde{z}_0}\right) - \Psi_m\left(\frac{z-d}{\tilde{L}}\right) + \Psi_h\left(\frac{\tilde{z}_0}{\tilde{L}}\right)}{\ln\left(\frac{z-d}{z_0}\right) - \Psi_m\left(\frac{z-d}{\tilde{L}}\right) + \Psi_h\left(\frac{\tilde{z}_0}{\tilde{L}}\right)} \tag{17}$$

$$T_* = \frac{-\tilde{H}_d}{c_p \cdot \tilde{\rho}_s \cdot u_*} \tag{18}$$

$$L = \frac{u_*^2 \cdot \tilde{T}_s}{\kappa \cdot g \cdot T_*} \tag{19}$$

Finally, aerodynamic resistance for each land use type has the following expression:

$$r_a(z) = \frac{1}{\kappa u_*}\left[\ln\left(\frac{z-d}{z_0}\right) - \Psi_m\left(\frac{z-d}{L}\right) + \Psi_h\left(\frac{z_0}{L}\right)\right] \tag{20}$$

The roughness length z_0 and is given in Table 1 for each land cover and two different periods of the year.

Table 1: Roughness lengths for each surface cover over the land. Units: m**.**

Surface type	Period of the year	
	October-May	May-September
Grass	0.03	0.03
Arable	0.005	0.1
Permanent crops	0.2	0.2
Coniferous forest	2.0	2.0
Deciduous forest	0.1	2.0
Urban	2.0	2.0
Desert	0.001	0.001
Ice	0.001	0.001
Other	0.01	0.02

For water surface the roughness length z_0 is calculated using Charnock's formula:

$$z_0 = 0.032 \cdot \frac{u_*^2}{g} \tag{21}$$

1.4.2 The quasi-laminar boundary layer resistance

The formula from Hicks *et al.* (1987) is used for calculating the quasi-laminar boundary layer resistance, r_b:

$$r_b = \frac{2}{\kappa u_*} \cdot \left(\frac{Sc}{Pr}\right)^{2/3} \tag{22}$$

where Sc and $Pr = 0.72$ are Schmidt and Prandtl Numbers, respectively. The Schmidt Number is defined as: $Sc = \nu / D_i$, with ν being kinematic viscosity of air (0.15 $cm^2\ s^{-1}$) and D_i the molecular viscosity of pollutant *i*. The Schmidt and Prandtl Number corrections for four gases in the MADE50 model are shown in Table 2.

Over sea surface, the quasi-laminar boundary layer resistance, r_b is calculated according to Hicks and Liss (1976):

$$r_b = \frac{1}{\kappa u_*} \cdot \ln\left(\frac{z_0}{D_i} \cdot \kappa u_*\right) \tag{23}$$

The quasi-laminar boundary layer resistance, r_b in Equation (A2.23) can be very large or even negative on the other side. Therefore, limits are imposed on the calculated dry deposition velocity, so that its minimum is 0 $m\ s^{-1}$ and maximum 0.1 $m\ s^{-1}$.

Table 2: Schmidt/Prandtl number correction and diffusion ratio for gases in the MADE50 model (D_{H2O}=0.21 $cm^2\ s^{-1}$)**.**

Compound	D_{H2O}/D_i	$(Sc/Pr)^{2/3}$
SO_2	1.9	1.34
NO_2	1.6	1.19
NH_3	1.0	0.87
HNO_3	1.9	1.34

1.4.3 Surface resistance

Surface resistance, r_s, in the MADE50 model is calculated for each land cover type according to the so called RIVM formula (Erisman *et al.*, 1994; Seland *et al.* 1995; Jakobsen *et al.*, 1996):

$$r_s = [(r_{inc} + r_{soil})^{-1} + r_{ext}^{-1} + (r_m + r_{stom})^{-1}]^{-1} \quad (24)$$

where different soil resistance parameterizations are used for the individual compounds. For the surface covered by vegetation:

- The stomata resistance - r_{stom} is the resistance against the transport through the stomata of leaves and needles.
- The mesophyll resistance - r_m is the resistance of the internal plant tissues against uptake or destruction (in terms of chemical reactions).
- The external surface resistance - r_{ext} is the resistance to the exterior plant parts against the uptake or destruction of the compound.
- The in-canopy aerodynamic resistance - r_{inc} is the resistance against transport of air through vegetation towards the soil and lower plant parts.
- The soil resistance - r_{soil} is the resistance against the destruction or absorption at the soil surface.

The original parameterization of the external surface resistance in Equation (24) has been further modified (Jakobsen *et al.*, 1996) so that the Wesley's approach is now used for calculating this term (Wesley, 1989). For surfaces not covered by vegetation or those which are covered by snow the total surface resistance is set equal to the soil resistance of the selected surface type.

Because of limited space we can not present a complete parameterization of each term in Equation (24) for all compounds. The full description of the surface resistance parameterization, as well as the discussion of different terms in Equation (24) can be found in (Jakobsen *et al.*, 1996; 1997).

1.4.4 Calculation of the average dry deposition velocity

For each compound, the average dry deposition is calculated separately for the dry and wet part of the model grid cell. The average dry deposition velocity, $\overline{v_d}$ over the entire grid cell is a weighted sum of the dry deposition velocities for the wet and dry part of the grid:

$$\overline{v_d} = \phi \cdot \sum_{l=1}^{N} a_l \cdot v_{d,l}^{wet} + (1-\phi) \cdot \sum_{l=1}^{N} a_l \cdot v_{d,l}^{dry} \quad (25)$$

where N is the number of land cover classes in the grid cell, a_l is the fraction of the land cover in the grid cell, $v_{d,l}^{wet}$ and $v_{d,l}^{dry}$ are the dry deposition velocities in the wet and dry part of the grid cell. The wet fraction of the grid - ϕ is equal to zero when the grid cell has not been affected by

precipitation in the last six hours. Otherwise, ϕ is equal to the maximum cloud cover fraction aggregated over the vertical column.

1.5 Parameterization of wet deposition

Parameterization of the wet deposition processes in the MADE50 model includes both in-cloud and sub-cloud scavenging of gases and particles.

Following Berge (1993b), in-cloud scavenging coefficient for gases and particles is calculated according to the following formula:

$$S = \frac{P}{W \cdot \Delta z} \tag{26}$$

where Δz is the height of the grid cell, W is cloud water (in kg of water m^{-3}) and P is precipitation released from the individual grid cell. The concentration change caused by wet deposition is expressed as:

$$\frac{\partial c}{\partial t} = -S \cdot f_{aq} \cdot c \tag{27}$$

where c is the total concentration (gas, particle in the aqueous phase) of the pollutant and f_{aq} is the fraction of the pollutant dissolved in the droplets. For SO_2, the f_{aq} can be calculated from the following relation:

$$f_{aq} = \frac{1}{1 + \frac{1}{K_N \cdot R \cdot T \cdot L}} \tag{28}$$

where K_N is the efficient Henry's law constant, R is the gas constant, T is temperature in K and L is the volume fraction of liquid water in the total volume of air. For all other soluble compounds, $f_{aq} = 1$ (Jakobsen *et al.*, 1996).

The sub-cloud deposition of gases is calculated as described in Jonson and Berge (1995):

$$\frac{\partial c}{\partial t} = -c \cdot \frac{\Lambda \cdot P}{\Delta z} \cdot \frac{1}{\rho_w} \tag{29}$$

where Λ is the sub-cloud scavenging coefficient for each gas as given in Table 1.3. In this Table, function $f(t) = \sin\{2\pi((t-80)/366)\}$ describes seasonal variation of the variable part of the scavenging ratio for SO_2 and t is expressed in Julian days.

Table 3: Sub-cloud scavenging coefficients for gases**.**

Gas	Scavenging coefficient - Λ
SO_2	$1.5 \cdot 10^5 + 5 \cdot 10^4 \cdot f(t)$
HNO_3	$7 \cdot 10^5$
NH_3	$7 \cdot 10^5$

Wet deposition rate for particles is described by the following relation (Berge, 1993a):

$$\frac{\partial c}{\partial t} = -A \cdot M \cdot E \cdot c \tag{30}$$

where $A = 5.2\ m^3\ kg^{-1}\ s^{-1}$, M is the mass of precipitation and E is the mean collection efficiency ($E = 0.1$). Precipitation mass M is calculated assuming a fall speed for the droplets equal to $5\ m\ s^{-1}$.

1.6 Chemical reactions for nitrogen and sulphur

A schematic illustration of the nitrogen and sulphur chemistry in the MADE50 model is shown in Figure 1.

The main part of the chemical reaction scheme in the model follows the scheme originally applied in Hov *et al.* (1988). A thorough description of the original scheme is also supplied in Barett *et al.* (1995). Compared to the original scheme, applied in the Lagrangian EMEP model (see Appendix A1) several changes have been made. The number of chemical components have been reduced from 10 to 9, as the 'unspecified' NO_3^- particle (particulate nitrate not in the form of ammonium nitrate i.e. sea salt particles) is no longer included. Furthermore, the oxidation of SO_2 to sulphate is parametrized as a function of cloud cover and water content. In addition, all reaction rates are updated according to more recent references (Atkinson *et al*., 1996).

Chemical evolution is calculated every 200 sec. for NO, NO_2, PAN, HNO_3, NH_4NO_3, $SO_4^=$ and $(NH_4)_{1.5}SO_4$. In addition to these, concentrations of ozone (O_3), hydroxyl (OH), peroxyacetol (CH_3COO_2) radicals and hydrogen peroxide (H_2O_2) are required for the chemical scheme. These are prescribed values described along with the boundary conditions in section A2.7.

Following Jakobsen *et al.*, (1997), all chemical reactions and reaction rates with references, are listed in Tables 4 and 5.

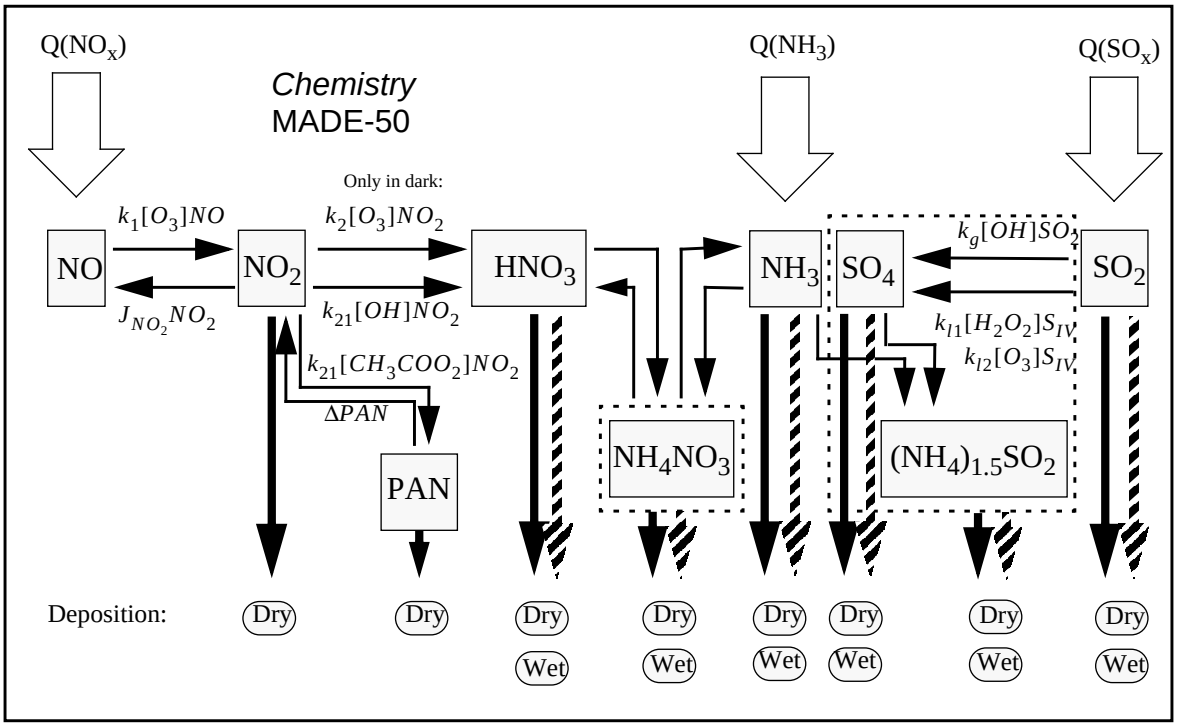

Figure A2.1. Schematic illustration of the MADE50 model chemical scheme. Dashed boxes denote nitrate and sulphate particles occurring in two forms. Solid and dashed thick arrows represent dry and wet deposition, respectively.

Table 4: Two-body reactions**.**

	Reaction	k_0	E_a/R	ref/note
R1	$NO_2+h\nu \rightarrow NO+O$			note[a]
R2	$NO+O_3 \rightarrow NO_2+O_2$	1.8×10^{-12}	1370	C/note[b]
R3	$2NO_2+O_3+H_2O \rightarrow 2NO_3^-+2H^++O_2$	1.2×10^{-13}	2450	C/see text
R4	$NH_4+HNO_3 \rightarrow NH_4NO_3$			see text
R5	$SO_2+ OH \rightarrow$ -------- sulphate	2.0×10^{-12}		C
R6	$3NH_4+2SO_4^{2-} \rightarrow 2\ (NH_4)_{1.5}SO_4^{2-}$			see text

a. Dissociation rate for NO_2: $J = 0.01 \times \exp(-0.39 \sec\theta)$, where θ is the solar zenith angle. Below clouds the dissociation rate is reduced by a factor of 0.5 times the fractional cloud cover.

b. Ozone concentrations from Berntsen (1994), see text.

For two-body reactions the temperature dependent rate constant (cm^3 $molecules^{-1}$ s^{-1}) given by: $k = k_0 \exp(-E_a/(RT))$ *and T is temperature in Kelvins. C is Atkinson et al. (1996).*

Table 5: Three-body reactions**.**

Reaction		k_0	k_∞	ref.
R7	$OH + NO_2 + M \rightarrow HNO_3 + M$	$2.6E\text{-}30(T/300)^{-2.9}N_2$	$6.7E\text{-}11(T/300)^{-0.6}$	A
R8	$NO_2 + CH_3COO_2 + M \rightarrow PAN + M$	$2.7E\text{-}28(T/300)^{7.1}N_2$	$1.2E\text{-}11(T/300)^{-0.9}$	A
R9	$PAN + M \rightarrow CH_3COO_2 + NO_2 + M$	$4.9E\text{-}3\ e^{(-12100/T)}N_2$	$4.0E+16\ e^{(-13600/T)}$	A

For 3-body reactions temperature and pressure dependant rate constants (cm^3 $molecules^{-1}$ s^{-1}) are given by

$$k = \left(\frac{k_0(T)M}{1 + k_0(T)M/(k_\infty(T))}\right) F_c^{\left(1 + (\log((k_0(T)M)/(k_\infty(T))))^2\right)^{-1}}$$

where M is the molecule density of air and T is temperature in Kelvins. F_c is 0.3 for R11, else 0.6, A is Atkinson et al. (1996).

Provided that the concentration of peroxy radicals is low, the ratio between NO and NO_2 is to a good approximation determined by the O_3 concentration through the reaction: R2: $NO + O_3 \rightarrow NO_2 + O_2$ and the photolytic reaction R1: $NO_2 + h\nu \rightarrow NO + O$.

Under clear sky conditions the dissociation rate for NO_2 (R7) is assumed constant in the vertical. Below clouds the dissociation rate is reduced by a factor of 0.5 times the fractional cloud cover. In particular over polluted areas in summer, the concentration of peroxy radicals can be significant. If so, the NO to NO_2 ratio is likely to be overestimated by the model.

PAN (peroxyacetylnitrate) is formed when NO_2 reacts with the peroxyacetyl radical (R8). In addition to dry deposition, PAN is thermally decomposed. The thermal decomposition is highly temperature dependent. In high latitudes in winter or in the upper troposphere, where temperatures are low, PAN is stable. As it is advected south (or down) it is thermally decomposed, acting as a reservoir for NO_2.

HNO_3 is produced from NO_2 The most important production term (especially in summer) is the reaction with OH (R7), giving HNO_3. The night time production of HNO_3 is assumed to be limited by the reaction $NO_2 + O_3 \rightarrow NO_3 + O_2$. This assumption only holds in the presence of a sufficient number of aerosols, and provided that the humidity is above the deliquescence point. (Platt, 1986; Dentener and Crutzen, 1993). The number of particles will usually decrease rapidly with height above the planetary boundary layer. Thus this reaction is assumed to take place in the lowest 8 layers of the model only (below approximately 1500 meters). This process is previously described in Jonson and Berge (1995), and the parameterization of this reaction will not be discussed further here. There are however large uncertainties related to this part of the chemistry scheme.

The formation of ammonium sulphate is assumed to occur instantaneously, only limited by the availability of NH_4 and SO_4^{2-}. Ammonium sulphate may exist in two forms, $(NH_4)_2SO_4$ or NH_4HSO_4. It is assumed that the concentrations of the two forms are equal.

Provided that NH_4 is in excess of sulphate, ammonium nitrate is formed. The formation of ammonium nitrate is dependant on temperature and relative humidity. This process is described in more detail in Hov *et al.* (1988). We first calculate the equilibrium concentration of NH_3:

$$NH_3eq = \frac{NH_3 - HNO_3}{2} + \sqrt{\left(\frac{NH_3 - HNO_3}{2}\right)^2 + k_{eq}} \tag{31}$$

The equilibrium concentration of NH_4HNO_3 is derived from NH_3:

$$NH_4NO_3eq = NH_4NO_3 + (NH_3 - NH_3eq) \tag{32}$$

Provided that the difference between the equilibrium concentration and the former concentration is smaller than the former concentration, the equilibrium concentration becomes the new concentration for ammonium nitrate. Ammonia and nitric oxide are adjusted accordingly. The equilibrium constant k_{eq} is determined as described below.

The Equilibrium reaction between HNO_3 and NH_4 (R6) is calculated according to the recommendations by Mozurkewich (1993). Below the point of deliquescence the equilibrium constant, K_p, is given by the equation:

$$\ln K_p = 118.87 + \frac{24084}{T} - 6.025\ln(T) \tag{33}$$

where T is the temperature in Kelvins. Above the point of deliquescence the equilibrium constant, now denoted K_{paq} is given by:

$$K_{paq} = \left[P_1 - P_2\left(1 - \frac{RH}{100}\right) + P_3\left(1 - \frac{RH}{100}\right)^2\right] \cdot \left(1 - \frac{RH}{100}\right)^{1.75} K_p \tag{34}$$

Both K_p and K_{paq} are in units of $(molecules\ cm^{-3})^2$. RH is the relative humidity in percent, and P_1, P_2 and P_3 are defined as:

$$\begin{aligned} \ln P_1 &= -135.94 + \frac{8763}{T} + 19.12\ln(T) \\ \ln P_2 &= -122.65 + \frac{9969}{T} + 16.22\ln(T) \\ \ln P_3 &= -182.61 + \frac{13875}{T} + 2446\ln(T) \end{aligned} \tag{35}$$

A2.6.1 Oxidation of SO_2

Within the clouds we assume that Henry's law applies:

$$[C] = H_c P_c \tag{36}$$

where $[C]$ is the concentration of any soluble gas C (*in mol* l^{-1}) in the aqueous phase, H_c its Henry's law coefficient and P_c the partial pressure of C in the gas phase. Within the aqueous phase many soluble gases undergo rapid reversible reactions such as acid-base ionization. It is therefore convenient to extend the definition above to an efficient Henry's law coefficient H^{eff}, referring to the total amount dissolved (Schwartz, 1986). Equilibrium reactions and solubility constants for these reactions are given in Table A2.6.

Table 6: Equilibrium reactions and solubility constants**.**

Reaction		K_{298}	ΔH/R	ref.
H_{SO2}	SO_2 g ↔ SO_2 aq	1.23	3020	1
K_1	SO_2 aq ↔ HSO_3^- + H^+	1.23 10^{-2}	2010	1
H_{H2O2}	H_2O_2 g ↔ H_2O_2 aq	7.1 10^4	6800	2
H_{O3}	O_3 g ↔ O_3 aq	1.13 10^{-2}	2300	3

K_{298} in mol l^{-1} atm^{-1} for Henry's law constants, and mol l^{-1} for aqueous phase equilibrium (K1). The temperature dependant rate is calculated by: $K = K_{298} \exp\left(-\left(\frac{\Delta H}{R}\right) \cdot (1/T - 1/298)\right)$

1) is Smith and Martell (1976), 2) is Martin and Damschen (1981) and 3) is Kozak-Channing and Helz (1983).

In the case of SO_2 the efficient Henry's law coefficient is defined as:

$$H_{SO2}^{eff} = \frac{S_{IV}}{P_{SO_2}} = H_{SO_2}\left(1 + \frac{K_1}{[H^+]} + \frac{K_1 K_2}{[H^+]^2}\right) \tag{37}$$

where S_{IV} is the total amount of dissolved SO_2.

In order to find an expression for the total concentration $[C_T]$ (gas and liquid - *mol* l_{air}^{-1}) we make use of the ideal gas law, $P_c = [C_g]RT$, where $[C_g]$ is the gas phase concentration of C (*mol* l_{air}^{-1}), R is the universal gas constant and T is temperature. Within the cloud the total concentration can be expressed as:

$$[C_T] = [C_{aq}]\left(1 + (H_c^{eff} \cdot R \cdot T \cdot clw)^{-1}\right) \tag{38}$$

and thus the fraction of the total mass remaining in the interstitial cloud air f_g and the fraction absorbed by the droplets can be calculated:

$$f_{aq} = \frac{[C_{aq}]}{[C_T]} = \frac{1}{1 + (H_c^{eff} \cdot R \cdot T \cdot clw)^{-1}} \quad \text{and} \quad f_g = 1 - f_{aq} \tag{39}$$

A2.6.1.1 Gas phase oxidation of SO_2

Within a grid cell the gas phase oxidation of SO_2 to sulphate (R5, Table A2.4) takes place both in the clouds and in the cloud free fraction of the grid cells. In cloudy air only the fraction of total SO_2 remaining in the gas phase is oxidized. We have found it convenient to define a pseudo reaction rate k_{12}^l, where the reaction rate is reduced instead of the concentration:

$$k_{12}^l = k_{12}(f_{g(so2)} cl + 1 - cl) \tag{40}$$

Thus the production of sulphate in the gas phase can be written $P_{SO2} = k_{12}^l \times SO_2(tot) \times OH$, where SO_2(tot) is the total (gas- and liquid-phase) concentration of SO_2.

A2.6.1.2 Aqueous phase oxidation of SO_2

In the aqueous phase we assume that SO_2 is oxidized to sulphuric acid by dissolved H_2O_2 and O_3 with the rate expression:

$$P_{cl} = k_{cl1}[H_2O_2][SO_2] + k_{cl2}[H^+][O_3]([SO_2] + [HSO^{-3}]) \tag{41}$$

where the reaction rate for oxidation by H_2O_2, $k_{cl1} = 8.3 \times 10^5$ $mol^{-1}l$ (Martin and Damschen, 1981) and the reaction rate for the oxidation by O_3, $k_{cl2} = 1.8 \times 10^4 [H^+]^{-0.4}$ $mol^{-1}l$ (Moller, 1980).

As we did for the gas phase production described above, we define pseudo reaction rates, taking into account the solubility of SO_2, H_2O_2 and O_3, the liquid water content and the fractional cloud cover.

$$k_{cl1}^l = \frac{k_{cl1} \times 10^3}{A_0 \cdot clw} \cdot \frac{H_{SO2}}{H_{SO2}^{eff}} \cdot f_S \cdot f_H \cdot cl \tag{42}$$

$$k^{l}_{cl2} = \frac{k_{cl2} \times 10^{3}}{A_0 \cdot clw} \cdot f_S \cdot f_{O3} \cdot cl \qquad (43)$$

where f_S, f_H and f_{O3} are the fraction of SO_2, H_2O_2 and O_3 dissolved in the droplets. Concentrations of ozone and hydrogen peroxide are prescribed. Ozone concentrations are prescribed (Jonson and Berge, 1995). Ozone concentrations are about 30 ppb_v in the boundary layer, increasing gradually with height to about 100 ppb_v in the upper troposphere.

In the aqueous phase the reaction between H_2O_2 and SO_2 is very fast, so that the least abundant of the two is depleted within a few minutes after the air enters the cloud. In order to simulate a reduction in the in-cloud hydrogen peroxide concentrations when SO_2 concentrations are high, hydrogen peroxide is reduced according to the expression:

$$H_2O^{l}_2 = \frac{H_2O_2 \times H_2O_2}{H_2O_2 + SO_2} \qquad (44)$$

where $H_2O^l_2$ denotes the total (gas and liquid) concentration of hydrogen peroxide in the cloud. Thus, whenever SO_2 is in excess of H_2O_2, the oxidation is reduced. The above formulations are likely to underestimate the rapid oxidation in newly formed clouds, and in parts of the clouds where dry air is entrained into the cloud. At the same time the oxidation can be overestimated in aged cloud environments with virtually no H_2O_2 left.

With the definitions above, the oxidation of SO_2 to sulphate in both gas- and aqueous phase can be expressed as:

$$P = (k^{l}_{12} \times OH + k^{l}_{cl1} \times H_2O_2 + k^{l}_{cl2} \times O_3) SO_2(tot) \qquad (45)$$

with total concentrations (gas and liquid) of SO_2(tot), H_2O_2, O_3 and OH given as *molecules* cm^{-3} air.

A2.7 Initial and boundary conditions

Initial boundary conditions for the model run assume zero concentrations of NO, NO_2, PAN, NH_3, HNO_3, NH_4NO_3, SO_4, SO_2 and $(NH4)_{1.5}SO_4$ in each grid cell of the model domain.

There are three types of the boundary conditions in the MADE50 model. Closed boundary conditions are used at the top of the model domain (100 hPa - at approximately 15 km). At the surface, the flux of pollutants to the ground is determined by dry deposition, wet deposition and emissions of SO_2, NO_x and NH_3. Open boundary conditions are used at lateral boundaries of the model domain. For sulphur, the lateral boundary concentrations are based on seasonally averaged concentrations from a hemispheric model (Tarrason and Iversen, 1996), and for NO, NO_2, HNO_3 and PAN on monthly averaged concentrations from the global Chemical Tracer

Model - CTM (Berntsen, 1994). Ozone concentrations, used in the chemistry calculations, are also taken from the global CTM. No inflow of ammonia concentrations is assumed through the lateral boundaries.

Concentrations of OH and CH_3COO_2 are prescribed by simple functions of the solar zenith angle, θ, as described in Table A2.7.

Table 7: Prescribed concentrations of OH and CH_3COO_2 in *molecules* cm^{-3}.

Compound	Night	Day
OH	10^4	$10^4 + 4\times10^6\exp(-0.25/\cos\theta)$
CH_3COO_2	10^5	$0.5\ (105 + 4 \times 10^6\exp(-0.25/\cos\theta)$

Also hydrogen peroxide concentrations have to be prescribed for the chemical part of the MADE50 model. These concentrations are highly variable both in space and time. H_2O_2 is produced by the reaction: $HO_2 + HO_2 \rightarrow H_2O_2 + O_2$. As the abundance of HO_2 depends on the photodissociation of ozone, hydrogen peroxide concentrations have a marked seasonal variation. In polluted areas (with high NO_x) HO_2 readily reacts with NO, reducing the production of hydrogen peroxide. In the model calculations we assume an annual average concentration of H_2O_2 of 0.35 ppb_v, with sinusoidal variation of 0.3 ppb_v and a maximum concentration in summer.

A2.8 Numerical grid system and meteorological input data

The model domain has been selected to cover area large enough to avoid the influence of boundary conditions on the meteorological parameters. This area covers not only Europe, which is of the main interest, but also a large part of the Atlantic Ocean from where air masses are very often coming to Europe.

The basic model Equation (A2.1) is solved in the numerical grid system which is shown together with the model domain in Figure A2.2. The EMEP area, where emissions are reported by European countries under the Convention on Long-Range Transboundary Air Pollution, is also shown in Figure A2.2. For each grid cell, emissions are computed as the annual sum from the entire grid cell. The vertical model structure is shown in Figure A2.3. Concentrations at each time step are computed in 20 sigma layers, in the centre of each three-dimensional grid cell. Usually 10 layers are placed below 2 km to obtain high resolution of the boundary layer where the most of the long range transport takes place. Three-dimensional grid system of the MADE50 model domain consists of 401 660 three-dimensional grid cells.

The MADE50 model requires very large amount of meteorological input data. To fulfil this requirement a special version of the Numerical Weather Prediction (NWP) model of the Norwegian Meteorological Institute LAM50E (Grønås and Midtbø, 1984; Nordeng, 1986) was run for the entire 1996. A more detailed information about the NWP models available at the Nor-

wegian Meteorological Institute for the EMEP purposes is given in Appendix A1.

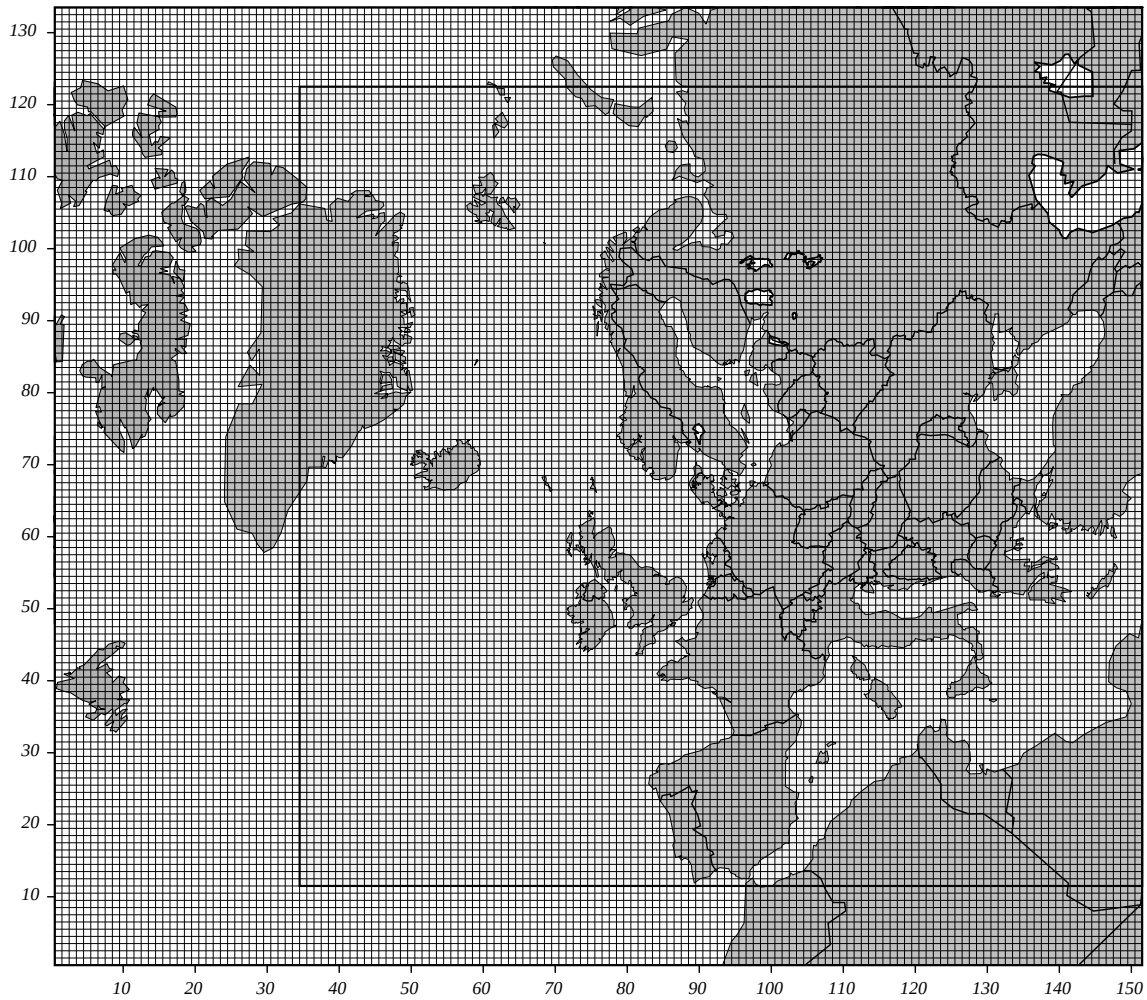

Figure A2.2. Horizontal domain and numerical grid of the MADE50 model. Grid size is 50 km at 60^{o}N. Emissions and meteorological input data are assigned to the centre of each 50 km x 50 km grid cell. Model output is computed in the same nodes. The EMEP region, in Figure A2.2, is marked with thick lines at the borders and shaded area inside.

Table 8: The most important meteorological input fields for the MADE50 model**.**

Field	Level	Field	Level
$\boldsymbol{U}$ - x-component of the wind	all levels	$\boldsymbol{P}$ - rate of precipitation release	all levels
$\boldsymbol{V}$ - y-component of the wind	all levels	$\boldsymbol{p_s}$ - surface pressure	surface
$\dot{\sigma}$ - vertical velocity in σ-coordinates	all levels	$\boldsymbol{Hs}$ - surface flux of sensible heat	surface
θ - potential temperature	all levels	$\boldsymbol{H_l}$ - surface flux of latent heat	surface
$\boldsymbol{q}$ - specific humidity	all levels	τ - surface stress	surface
$\boldsymbol{c_w}$ - cloud water	all levels	$\boldsymbol{T_{2m}}$ - temperature at 2 m	surface

For generating meteorological data, the LAM50E model was run for 12 hourly intervals, producing meteorological data for the last six hours of the forecast. The most important meteorological input fields for the MADE50 model are listed in Table A2.4. Meteorological input data for all 3-D grid cells of the MADE50 model are updated every six hour and linearly interpolated in time during the model run.

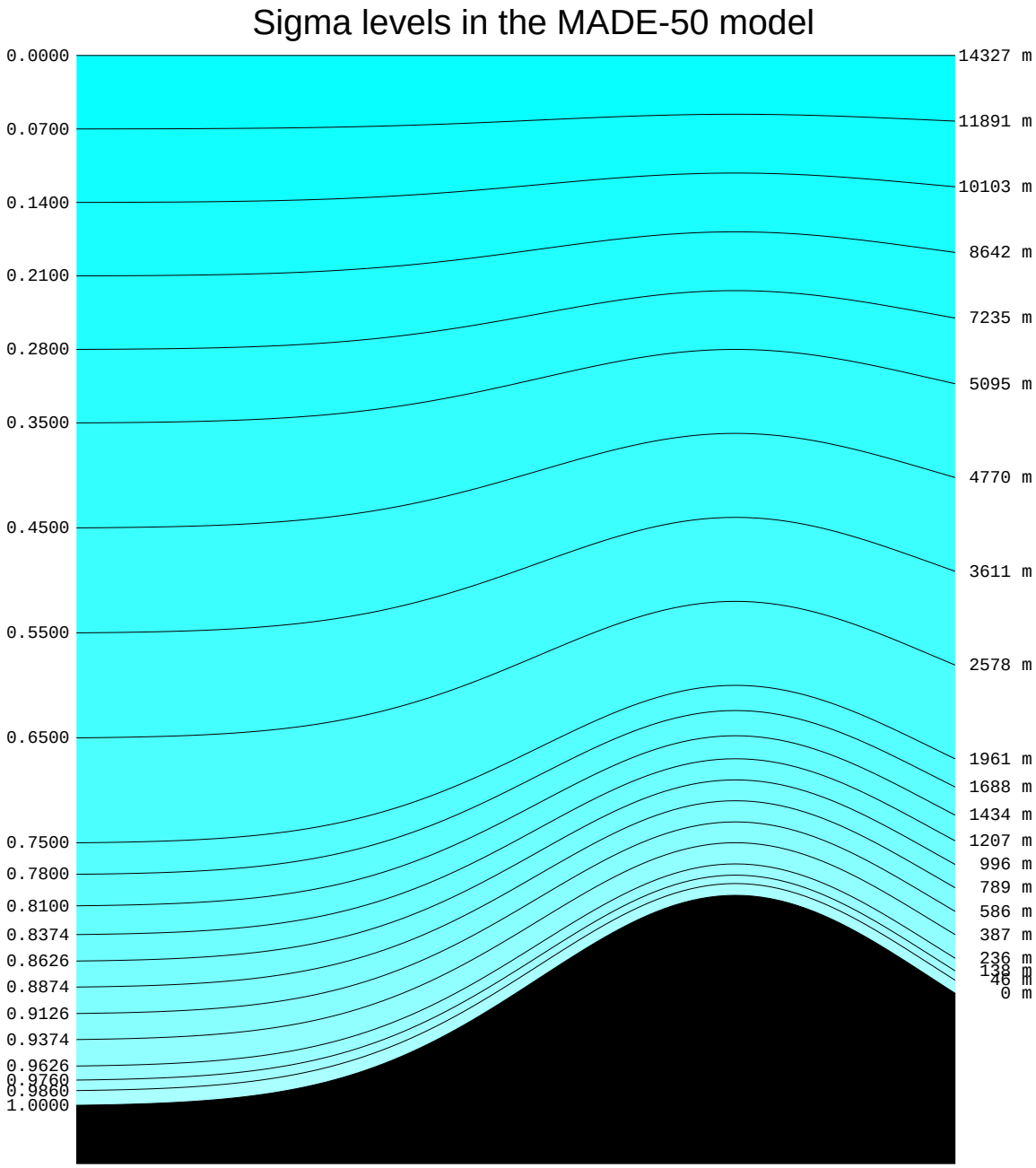

Figure A2.3. Vertical structure of the MADE-50 model. The troposphere is represented in the model by 20 sigma layers. Sigma values for each level are shown on the left hand side of the figure. The corresponding height above the ground, computed for the standard atmosphere, is given on the right hand side.

A2.9 Numerical solution of the model equations

Main model Equation A2.1 is solved numerically by using fractional time step method (McRae *et al.*, 1982). In this approach, different physical and chemical processes are represented by separate numerical operators which are successively applied by intermediate time integrations. A central-difference scheme is applied for space discretization of the vertical diffusion and Bott's method for the numerical approximation of horizontal and vertical advection.

From the numerical point of view, solution of the advection part of Equation A2.1 is the most difficult and requires an efficient and well tested algorithm. The chosen algorithm, developed by Bott (1989a, 1989b), is mass conserving, positive definite and fast in application. A fourth order version of this algorithm is used for the horizontal components of the velocity field and the second order, irregular grid version for the vertical component. The version of Bott's algorithm applied for the vertical advection has been developed at MSC-W in collaboration with Bott.

Time step in the model computations is equal to 10 minutes and is mainly limited by the vertical advection The Courant Number is checked every time step during the model run and when it exceeds one, the time step for the vertical advection and diffusion is reduced to five minutes. For the 1996 meteorology it was found to be a sufficient solution.

A2.10 Computer implementation and performance of the model

One year simulation with the latest version of the MADE50 model would requires weeks of CPU time on traditional sequential supercomputers. Therefore, the model was implemented on the parallel CRAY T3E computer in Trondheim - Norway. Theoretical and practical details about the parallelization and computer implementation of the model can be found in Skålin *et al.*, (1995). Below, we present some results from the model performance analysis.

Computational efficiency of the model was analysed introducing time measurements for the main segments of the code by means of irtc()-calls. Test runs have been done for a real time period of 1 day, i.e. nterm=5 was set and consequently 4 steps of 6 hours were done. Runs were performed on 4, 8, 16, 24 and 32 processors, assuming a fixed decomposition into 4 parts in the y-direction and a decomposition into 1, 2, 4, 6, 8 parts respectively in the x-direction. The higher number of processors in the x direction was chosen, since the total number of points in this direction (151 grid points) better fits a division into 8 parts than the number of points in the y-direction (133 grid points).

From the measured time characteristics of the model one comes to the following conclusions: 1. There is a super linear speed-up of the whole model for up to 32 processors relative to the 4 processors run. 2. This super linear speed-up comes mostly from the vertical advection/diffusion part (speed-up of 9.92 of 32 processors with respect to 4 processors) and from the chemistry solver (speed-up of 14.45 of 32 processors with respect to 4 processors). 3. These two parts of the program require the largest part of the CPU-time of the model (about 60% for a 4 processor run and 41% for a 32 processor run). The two other parts requiring large fraction of the CPU-time (horizontal advection and preparation of the rates and coefficients for the chemistry solver (together 34% for 4 processors and 35.5% for 32 processors) have a nearly linear scaling

factor. Consequently, to shorten the computation time of the model one has to look a little bit closer at the advection modules and the chemistry solver.

The advection is done by a fourth order Bott-scheme in the horizontal and a second order Bott-scheme in the vertical. A considerable part of the calculations in these schemes is independent of the actual species to be transported. This part of computations had been done separately for each species in the previous version of the model. These subroutines were reformulated to perform as much as possible calculations only once for all species. The computed direction dependent fluxes were subsequently applied to all species in one pass. Here arises another problem: In the original formulation the concentration array had the structure of indices (i,j,k,n), consequently, the species dependent coordinate 'n' was the slowest varying index. To avoid introduction of large additional 3D arrays for the fluxes, etc. and to hold the structure of the advection routines as it is (with local 1D or 2D arrays - one geometric dimension + species dimension) the order of indices in the concentration array has been changed to (n,i,j,k). Since now the species dependent index is the fastest varying, the loop over the species can be the inner most, the inflow/outflow tests in the advection routine can be moved out of this loop and the code can be highly optimized by the compiler. The resulting horizontal advection code is about 5 times faster than the old one, the vertical advection/diffusion code, which allowed, in addition, other optimization steps, became more than 10 times faster in the 4 processors case and more than 8 times faster in the 32 processors case. Of course, the high super linear speed-up now disappeared, it remains only small super linear speed-up in the advection in the y-direction (second geometric coordinate) and vertical advection (third geometric coordinate) coming from the fact, that the program has to access data in the memory, which are separated by smaller strides for higher processor numbers.

The same reordering of indices in the concentration array improves performance of the chemistry solver and of the preparation phase, too, since now concentration values for one point of the domain lay in the memory one after another and are much faster to access. The super linear speed up came mainly from the following: The solver solves at once the chemical equations for one horizontal line. If this line is too long, the arrays do not fit into cache leading to cache conflicts. A length of about 20 for 32 processors gives a performance improvement of nearly a factor of 2 compared with the length 150 for a 4 processor run.

In addition, chemistry system has to be solved in the inner part of the domain only, leading to the fact, that the lower/upper bounds of the arrays are not known at compile time avoiding the compiler from doing maximum possible optimization. Here following change has been done: computation line is now a vertical line. This may lead to a little bit decreasing performance in the copying phase of concentrations to working arrays, but it is more than repaid by the fact, that now lower and upper bounds of the arrays are known at compile time (and are independent of the number of processors). In the preparation of coefficients for the solver large time is spent in computing power functions. Since the corresponding powers and bases are clearly away from zero, the power function *x**y* can be replaced by *exp(y*log(x))* which is much faster. This all together results in 3 times faster execution of the chemistry in the new model.

The resulting computation time for the new version of the whole model is more than 4 times shorter for the 4 processors case and more than 3 times shorter in the 32 processors case. The high super linear speed-ups disappear indicating that the new program makes better use of the cache already for smaller processor numbers. The speed-up characteristics of the program, consequently, are smaller now, nevertheless remaining quite high: For the part executed at each time step speed-up for 32 processors with respect to 4 processors is 7.4, the advection shows

slight super linear speed-up of 8.08. The results of the computational model performance analysis are illustrated in Figure A2.4.

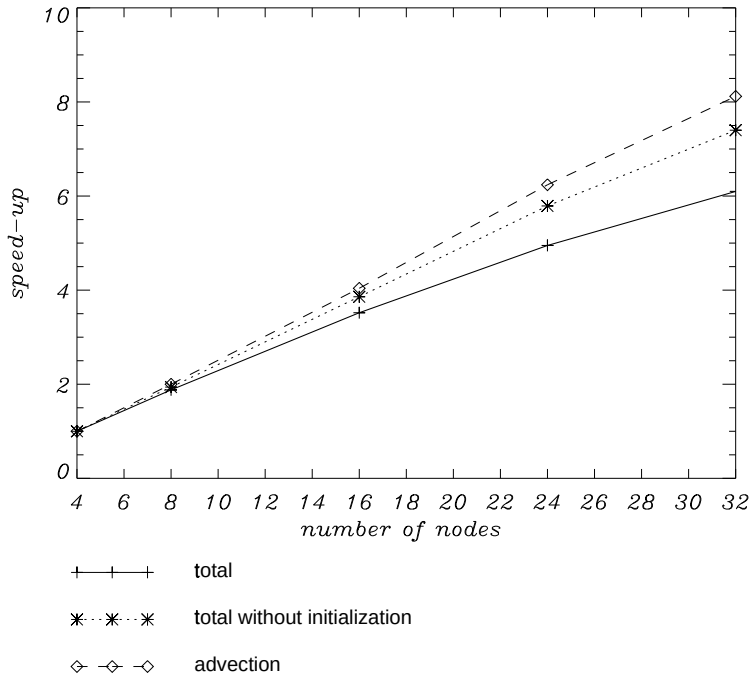

Figure A2.4. Speed-up factor for the MADE50 model parallel computations as a function of a number of processors involved in the computations.

From a practical point of view the main conclusion is the following: A computation, which required in the past the use of 32 processors can now be done on 8 processors in even somewhat shorter time. A one months run can be performed in 90 minutes on 8 processors.

References

Atkinson R., Baulch D.L., Cox R.A., Hampson R.F., Kerr J.A and J. Troe (1992) Evaluated kinetic and photochemical data for atmospheric chemistry. Supplement IV, IUPAC subcommittee on gas kinetic data evaluation for atmospheric chemistry. *Atmospheric Environment*, **26A**, 1197-1230.

Barret K., Seland Ø., Mylona S., Foss A., Sandness H., Styve H. and L. Tarrason (1995) European transboundary acidifying air pollution. Ten years calculated fields and budgets to the end of the first Sulphur Protocol. EMEP/MSC-W Report 1/95. The Norwegian Meteorological Institute, Oslo, Norway.

Barret K. and E. Berge (1996) Transboundary Air Pollution in Europe. EMEP/MSC-W Report 1/96. The Norwegian Meteorological Institute, Oslo, Norway.

Berge E. (1993a) Preliminary estimates of sulphur transport and deposition in Europe with a regional scale multi-layer Eulerian model. EMEP/MSC-W Note 1/93. The Norwegian Meteorological Institute, Oslo, Norway.

Berge E. (1993b) Coupling of wet scavenging of sulphur to clouds in a numerical weather prediction model. *Tellus* **45b**, 1-22.

Berge E. (1997) Transboundary Air Pollution in Europe. MSC-W Status Report 1997. Part 1 and 2. EMEP/MSC-W Report 1/97. The Norwegian Meteorological Institute, Oslo, Norway.

Berge E. and H.A. Jakobsen (1998) A regional scale multi-layer model for the calculation of long term transport and deposition of air pollution in Europe. Submitted and accepted to *Tellus*.

Berntsen T. (1994) Two- and three-dimensional model calculations of photochemistry of the troposphere. Ph.D. Thesis. Department of Geophysics, University of Oslo, Norway.

Blackadar A.K. (1979) High resolution model of the planetary boundary layer. *Advances in Environmental and Scientific Engineering, 1.* Gordon and Branch, 276 pp.

Bott A. (1989a) A positive definite advection scheme obtained by non-linear renormalization of the advective fluxes. *Monthly Weather Review* **117**, 1006-1015.

Bott A. (1989b) Reply. *Monthly Weather Review* **117**, 2633 - 2636.

Dentener F.J. and P.J. Crutzen (1993) Reaction of N_2O_5 on tropospheric aerosols: Impact on the global distributions of NO_x, O_3 and OH. *J. Geophys. Res.* **98**, 7149-7163.

Erisman J. W., van Pul W.A.J. and G.P. Wyers (1994) Parameterization of surface resistance for the quantification of atmospheric deposition of acidifying pollutants and ozone. *Atmospheric Environment* **28(16)**, 2595-2607.

Grønås, S. and K.H. Midtbø (1984) Operational multivariate analysis by successive corrections. *J. Meteo. Soc. Japan* **65**, 61 - 74.

Hicks B.B., Baldocchi D.D., Mayers T.P., Hosker R.P. Jr. and D.R. Matt (1987) A preliminary multiple resistance routine for deriving dry deposition velocities from measured quantities. *Water Air and Soil Pollution*, 36, pp. 311-330.

Hicks B.B., Liss P.S. (1986) Transfer of SO_2 and other reactive gases across the air-sea interface. *Tellus* **36**, 311-330.

Hov Ø. Eliassen A. and D. Simpson (1988) Calculation of the distribution of NO_x compounds in Europe. In: *Tropospheric Ozone - Regional and Global scale Interactions* (I.S.A Isaksen ed.). Reidel Publishers, Dordrecht, pp. 217-239.

Jakobsen H.A., Berge E., Iversen T. and R. Skålin (1995) Status of the development of the multilayer Eulerian model. a) Model description; b) New method for calculating mixing heights; c) model results for sulphur transport and deposition in Europe for 1992 in the 50 km grid. EMEP/MSC-W Note 3/95. The Norwegian Meteorological Institute, Oslo, Norway.

Jakobsen H. A., Jonson, J. E., Berge, E. (1996) Transport and deposition calculations of sulphur and nitrogen compounds in Europe for 1992 in the 50 km grid by use of the multi-layer Eulerian model. EMEP/MSC-W Note 2/96. The Norwegian Meteorological Institute, Research Report no 34, The Norwegian Meteorological Institute, Oslo, Norway.

Jakobsen H.A., Jonson J.E. and E. Berge (1997) The multi-layer Eulerian model: Model description and evaluation of transboundary fluxes of sulphur and nitrogen for one year. EMEP/MSC-W Note 2/97. The Norwegian Meteorological Institute, Oslo, Norway.

Jonson J.E., Bartnicki J., K. Olendrzynski, H.A. Jakobsen and E. Berge (1998a). EMEP Eulerian model for atmospheric transport and deposition of nitrogen species over Europe. Accepted to *Environmental Pollution*.

Jonson J.E., K. Olendrzynski, Bartnicki J., H.A. Jakobsen and E. Berge (1998a). EMEP Eulerian model for acid deposition over Europe. Preprints of the 5th international Conference on Harmonization within Atmospheric Dispersion Modelling for Regulatory Purposes. May 1998, Rhodes, Greece.

Jonson J.E., and E. Berge (1995). Some preliminary results on transport and deposition of nitrogen compounds by use of multi-layer Eulerian model. EMEP/MSC-W Note 1/95. The Norwegian Meteorological Institute, Oslo, Norway.

Kozak-Channing L.F. and G.R. Helz (1983) Solubility of ozone in aqueous solutions of 0-0.6 M ionic strength at 5-30 C. *Envir. Sci. Technol.,* **17**, 145-149.

Luis J.F. (1979) A parametric model for vertical eddy fluxes in the atmosphere. *Boundary Layer Meteorology,* **17**, 187-202.

Martin L.R. and D.E. Damschen (1981) Aqueous oxidation of sulphur dioxide by hydrogen peroxide at low pH. *Atmospheric Environment,* **15**, 1615-1621.

McRae G.J, Goodin W.R and J.H. Seinfeld (1982) Numerical solution of the atmospheric diffusion equation for chemically reacting flows. Journal of Computational Physics, 45,1-42.

Moller D. (1980) Kinetic model of atmospheric SO_2 oxidation based on published data. *Atmospheric Environment,* **14,** 1067-1076.

Mozurkewich M. and J.G. Calvert (1988). Reaction probability of N_2O_5 on aqueous aerosols. *J. Geophys. Res.,* **93**, 15.889-15.896.

Nordeng T.E. (1986) Parameterization of physical processes in a three-dimensional numerical weather prediction model. DNMI Technical Report No. 65. Norwegian Meteorological Institute, Oslo, Norway.

Olendrzynski K., Bartnicki J., and J. E. Jonson (1998) Prformance of the Eulerian Acid deposition Model. In: *Transboundary Acidifying Air Pollution in Europe. MSC-w Status Report 1998 - Part 1: Estimated dispersion of acidifying and eutrophying compounds and comparison with obsrvations*. EMEP/MSC-W Report 1/98. The Norwegian Meteorological Institute, Oslo, Norway.

Platt U. (1986). The origin of nitrous and nitric acid in the atmosphere. *Chemistry of muliphase atmospheric systems*. Edited by W. Jaeschke, Nato ASI Series G, Vol. 6, Springer Verlag, Berlin, pp. 299-321.

Schwartz S.E. (1986) Mass-transport considerations pertinent to aqueous phase reactions of gases in liquid-water clouds. *Chemistry of multiphase atmospheric systems*, Ed. by W. Jaeschke, Springer-Verlag, Berlin, pp 415-471.

Skålin R., Lie I. and E. Berge (1995). A parallel algorithm for simulation of long range transport of air pollution. In: *High Performance Computing in Geosciences* (F.X. Le Dimet ed.), Kluwer Academic Publishers, Dordrecht, The Netherlands, pp. 175-185.

Seland Ø., van Pul A. Sorteberg A. and J.P. Tuovinen (1995) Implementation of a resistance dry deposition module and a variable local correction factor in the Lagrangian EMEP model. EMEP/MSC-W Report 3/95. The Norwegian Meteorological Institute, Oslo, Norway.

Smith R.M. and A.E. Martell (1976) *Critical stability constants*, Vol. 4, Inorganic complexes, Plenum Press, New York.

Tarrason L. and T. Iversen (1998) Sulphur dispersion in northern hemisphere: Simulations with a 3-dimensional time-resolved model. *Tellus*, (in print).

Wesely M. L. (1989) Parameterization of surface resistances to gaseous dry deposition in regional-scale numerical models. *Atmospheric Environment*, **23**, 1293-1304.

Smith R.M. and A.E. Martell (1976) Critical stability constants, Vol. 4, inorganic complexes, Plenum Press, New York.